Article type   : Original

Hedgehog signaling modulates IL-33-dependent extrahepatic bile duct cell proliferation in mice

Nataliya Razumilava[1*]

Junya Shiota[1]

Nureen H. Mohamad Zaki[1]

Ramon Ocadiz-Ruiz[1]

Christine M. Cieslak[1]

Kais Zakharia[1]

Benjamin L. Allen[2]

Gregory J. Gores[3]

Linda C. Samuelson[1,4]

Juanita L. Merchant[1,4]

Departments of [1]Internal Medicine, [2]Cell and Developmental Biology, [4]Molecular and Integrative Physiology, University of Michigan, Ann Arbor, MI; [3]Department of Internal Medicine, Mayo Clinic, Rochester, MN

*Address for Correspondence: Nataliya Razumilava, M.D.

109 Zina Pitcher Place

Biomedical Science Research Building, Room 2062

Ann Arbor, MI 48109

Tel: +1-734-764-5865

Fax: +1-734-763-4686

E-mail: razumila@med.umich.edu

Abbreviations: BD, bile duct; BDO, bile duct organoid; BEC, biliary epithelial cell; BrdU, 5-Bromo-2′-deoxyuridine; CK19, cytokeratin 19; DAPI, 4′,6-diamidino-2-phenylindole; EdU, 5-ethynyl-2′-deoxyuridine; EHBD, extrahepatic bile duct; GLI, glioma-associated oncogene; HA, hemagglutinin; HH, hedgehog; IHH, Indian hedgehog; IL-6, interleukin-6; IL-33, interleukin-33; NF-κB, nuclear factor-κB; PBG, peribiliary gland; PBS, phosphate-buffered saline; PTCH1, Patched1; RT, room temperature; SHH, Sonic hedgehog; ST2, suppression of tumorigenicity 2

Conflict of Interest: The authors have nothing to disclose.

ABSTRACT

Background and Aims: Hedgehog (HH) signaling participates in hepatobiliary repair after injury and is activated in patients with cholangiopathies. Cholangiopathies are associated with bile duct (BD) hyperplasia, including expansion of peribiliary glands, the niche for biliary progenitor cells. The inflammation-associated cytokine interleukin (IL)-33 is also up-regulated in cholangiopathies, including cholangiocarcinoma. We hypothesized that HH signaling synergizes with IL-33 in acute inflammation-induced BD hyperplasia. **Methods:** We measured extrahepatic BD (EHBD) thickness and cell proliferation with and without an IL-33 challenge in wild-type mice, mice overexpressing Sonic HH (*pCMV-Shh*), and mice with loss of the HH pathway effector glioma-associated oncogene 1 (*Gli1*$^{lacZ/lacZ}$). *LacZ* reporter mice were used to map the expression of HH effector genes in mouse EHBDs. An EHBD organoid (BDO) system was developed to study biliary progenitor cells *in vitro*. **Results:** EHBDs from the HH overexpressing *pCMV-Shh* mice showed increased epithelial cell proliferation and hyperplasia

when challenged with IL-33. In *Gli1*$^{lacZ/lacZ}$ mice, we observed a decreased proliferative response to IL-33 and decreased expression of *Il6*. The HH ligands *Shh* and *Ihh* were expressed in epithelial cells, while the transcriptional effectors *Gli1*, *Gli2*, and *Gli3* and the HH receptor Patched1 (*Ptch1*) were expressed in stromal cells, as assessed by *in situ* hybridization and *lacZ* reporter mice. Although BDO cells lacked canonical HH signaling, they expressed the IL-33 receptor suppression of tumorigenicity 2 (ST2). Accordingly, IL-33 treatment directly induced BDO cell proliferation in an NF-κB-dependent manner. **Conclusion:** HH ligand overexpression enhances EHBD epithelial cell proliferation induced by IL-33. This pro-proliferative synergism of HH and IL-33 involves crosstalk between HH ligand-producing epithelial cells and HH-responding stromal cells.

INTRODUCTION

The Hedgehog (HH) pathway plays a role in hepatobiliary inflammation and injury-related cancers. HH signaling involves Sonic hedgehog (SHH) and Indian hedgehog (IHH) ligands, the receptor Patched-1 (PTCH1), and their transcriptional effectors, glioma-associated oncogene 1 (GLI1), GLI2, and GLI3.[1] In the canonical HH pathway, cells expressing HH ligand signal to stromal cells expressing PTCH1 and GLIs in a variety of gastrointestinal tissues.[2-4] In the liver, HH ligands are expressed in both epithelial cells and myofibroblasts after injury, and HH signaling is responsible for the "reactive" phenotype of injured cholangiocytes.[5, 6] Prior studies, including from our group, suggest that HH signaling contributes to the initiation and progression of cholangiocarcinoma.[7, 8] However, most studies describing HH signaling in hepatobiliary pathology have focused on hepatocytes, intrahepatic BDs, and fully developed cancer. This work focuses on the effects of activated HH signaling on extrahepatic BDs (EHBDs) in acute inflammation.

Cholangiopathies represent a group of chronic progressive diseases affecting biliary epithelial cells (BECs). Cholangiopathies, which include primary sclerosing cholangitis and cholangiocarcinoma, are associated with inflammation and fibrosis.[9] Peribiliary glands (PBGs) are a specialized BEC compartment that contains biliary progenitor cells and participates in the maintenance and repair of large BDs.[10, 11] PBGs contain mature and immature cell types and proliferate in response to BD injury in experimental mouse models of biliary atresia and BD obstruction.[10] In humans, PBG hyperplasia is observed in numerous hepatobiliary pathologies,

including cholangitis, cirrhosis, and hepatic necrosis, likely representing a compensatory mechanism after biliary injury to replace damaged BD epithelium.[12] In patients with primary sclerosing cholangitis, increased HH signaling is associated with hyperplastic PBGs, dysplastic BD lesions, and advanced fibrosis.[13] The mechanisms underlying HH regulation of EHBD, and BEC and PBG epithelial hyperplasia have not been well described.

In children with biliary atresia, mRNA expression of the inflammatory cytokine interleukin-33 (*Il33*) and its receptor suppression of tumorigenicity 2 (*St2*) is increased in the liver, and IL-33 is increased in serum.[14, 15] Overexpression of IL-33 was described in patients with inflammatory cholangiopathies,[16] including hepatobiliary parasitic infection clonorchiasis[17] and visceral leishmaniasis,[18] and viral hepatitis B[19] and C[20]. The pro-oncogenic effect of IL-33 was recently described in a mouse model of cholangiocarcinoma, where biliary injury–induced IL-33 cooperated with KRAS and TGFβR2 mutations in the development of cholangiocarcinoma originating from PBGs.[21] Moreover, it was recently shown that IL-33 is a potent biliary mitogen, and IL-33–mediated proliferation of cholangiocytes was found to occur in a paracrine manner through IL-13 secretion from nearby type 2 innate lymphoid cells responding to IL-33.[15] Furthermore, when coupled with the oncogenes AKT and YAP, IL-33 promotes cholangiocarcinoma in mouse, which involves an interleukin-6 (IL-6)–sensitive mechanism.[22] In addition to IL-6 regulation by IL-33, HH signaling and, specifically GLI1, were reported modulate IL-6 expression in pancreatic cancer and stomach pre-neoplastic lesions.[2, 23]

These studies suggest a potential synergism between cell survival pathways and inflammation-induced cytokines in cholangiocyte proliferation. In this report, we tested whether activated HH ligand signaling accelerates epithelial cell proliferation in EHBDs after an inflammatory challenge with IL-33.

MATERIALS AND METHODS

Animal Experiments. All mouse experiments were approved by the University of Michigan's Institutional Animal Care and Use Committee. Transgenic *Shh* mice (*pCMV-Shh*) and *Gli1*[lacZ/lacZ] mice have been described.[2, 4, 27] The *Gli1*[lacZ./+] and *Gli1*[lacZ./lacZ] mice contain a knock-in *lacZ*, encoding a nuclear-localized β-galactosidase, into exon 2 of the mouse *Gli1* gene, producing a null allele.[28] The *pCMV-Shh; Gli1*[lacZ/+] and *pCMV-Shh; Gli1*[lacZ/lacZ] mice were generated by

crossing *pCMV-Shh* and *Gli1$^{lacZ/lacZ}$* mice. The *Gli2$^{lacZ/+}$*, *Gli3$^{lacZ/+}$*, and *Ptch1$^{lacZ/+}$* reporter mice were described.[29-32] All *lacZ* reporter mice were maintained on a mixed C57BL/6J; 129S4/SvJaeJ background. Mice were housed in a specific pathogen-free environment with a 12:12-hour light-dark cycle in ventilated caging and provided Enviro-Dri absorbent, cotton squares or cardboard tubing as enrichment. Animals were provided with free access to food (Purina LabDiet 5L0D; St Louis, MO, USA) and water. Recombinant mouse carrier free IL-33 (R&D Systems, Minneapolis, MN, USA) was reconstituted at 1 μg/100 μL in sterile phosphate-buffered saline (PBS). During the light cycle, adult male and female mice were given intraperitoneal injections of either PBS (100 μL) or IL-33 (1 μg) daily for 4 days, and tissues were isolated on day 5. Animals were euthanized during the light cycle with isoflurane combined with the removal of a vital organ according to institutional guidelines. Experimental replicates were sex and age matched as well as littermate matched when possible.

Human Samples. Human EHBD tissue from cholangiocarcinoma and adjacent non-cancerous bile duct was collected with the approval of the University of Michigan's Institutional Review Board according to the principles embodied in the Declaration of Helsinki. Paraffin embedded tissue was sectioned at 4 μm for further studies.

Immunohistochemistry. Mouse EHBDs were isolated and fixed in 10% formalin overnight at 4°C and then transferred to PBS before paraffin embedding. Human and mouse tissue sections (4 μm) were deparaffinized and rehydrated in serial xylene and alcohol dilutions and incubated in boiling citrate buffer (10 mM, pH 6) for 30 minutes for antigen retrieval. After antigen retrieval, slides were incubated in a 1% bovine serum albumin/5% fetal bovine serum/0.1% Triton-X-100-PBS blocking solution for 1 hour at room temperature (RT). Primary and secondary antibodies (Table 1) were diluted in the blocking solution. Tissue was incubated in primary antibodies overnight at 4°C and secondary antibodies for 1 hour at RT. ProLong Gold antifade reagent with 4′,6-diamidino-2-phenylindole (DAPI) (Life Technologies, Waltham, MA, USA) was used for nuclear counterstaining. Eosin (Thermo Fisher Scientific) was used for cytoplasmic staining, hematoxylin (Thermo Fisher Scientific) was used as a nuclear counterstain, and Permount (Thermo Fisher Scientific) was used as a mounting medium for hematoxylin and eosin (H&E)

staining of deparaffinized and rehydrated slides. Images were taken on Olympus BX53 and Nikon Eclipse E800 microscopes (Tokyo, Japan).

Histological stains. For X-gal staining, mouse EHBD was dissected, washed in ice-cold PBS, and fixed in cold 4% paraformaldehyde (PFA)-PBS for 1 hour before being washed in X-gal wash buffer (1 M $MgCl_2$, 2% NP-40, 0.1 M sodium phosphate buffer pH 7.3) three times at RT on a rocker. Tissue was then stained overnight at 37°C in the dark with 1 mg/mL of X-gal substrate (Roche, Basel, Switzerland) in 5 mM $K_3Fe(CN)6$, 5 mM $K_4Fe(CN)6 \cdot 3H_2O$, 2 mM $MgCl_2$, 0.02% NP-40, 0.1% deoxycholate buffer. After staining, samples were washed for 30 minutes, postfixed in 4% PFA at 4°C overnight, paraffin embedded, sectioned at 4 μm, deparaffinized, counterstained with Nuclear Fast Red (Sigma-Aldrich, St Louis, MO, USA) for 30 minutes, rinsed in tap water, dehydrated in alcohol dilutions, and mounted with Permount (Thermo Fisher Scientific).

In situ hybridization (RNAscope). Mouse EHBD formalin-fixed paraffin-embedded sections (5 μm) were deparaffinized and rehydrated in Histoclear (National Diagnostics, Atlanta, GA, USA) and 100% ethanol, followed by 10 minutes of incubation in H_2O_2 (RNAscope Pretreatment Reagents, ACD, Newark, CA, USA, catalog #322330). Next, slides were incubated in RNAScope Target Retrieval Reagent (ACD, catalog #322000) for 15 minutes at 95°C, rinsed with water and 100% ethanol, and treated with RNAScope Protease Plus (ACD) for 30 minutes at 40°C. Slides were then incubated with RNAScope probes (Negative control [ACD, catalog #310043], Mm-Shh [ACD, catalog #314361], Mm-Ihh [ACD, catalog #413091], or Mm-Gli1 [ACD, catalog #311001]) for 2 hours, with signal amplification using RNAscope 2.5 HD Detection Reagent (ACD) for 60 minutes at 40°C with washes using RNAscope Wash Buffer (ACD). Slides were incubated with 3,3′-Diaminobenzidine (DAB) for 10 minutes, counterstained with 1:8 Harris' hematoxylin (Thermo Fisher Scientific), dehydrated in graded ethanol and Histoclear (National Diagnostics) and mounted with Permount (Thermo Fisher Scientific).

Biliary proliferation. Proliferating cells were labeled by 5-Bromo-2′-deoxyuridine (BrdU) incorporation (50 mg/kg, intraperitoneally, 2 hours before tissue collection). The PBG and BEC areas were identified by cytokeratin 19 (CK19) immunostaining. Epithelial versus stromal cell

proliferation was measured using ImageJ software (National Institutes of Health, Bethesda, MD, USA, https://imagej.nih.gov/ij/) by an author blinded to experimental conditions.

Morphometrics. Each EHBD section was analyzed for BD wall thickness (excluding lumen) at three points 100 µm apart. Only sections with well-aligned BD lumen and wall were used for analysis. Organoid growth was monitored by taking pictures with an inverted Leica DM IRB microscope (Wetzlar, Germany) using an Olympus DP7 (Tokyo, Japan) camera. The area occupied by organoids was measured with ImageJ software.

Quantitation of SHH ligand. Blood was collected by cardiac puncture and serum was isolated. SHH ligand levels were measured with a spectrophotometric enzyme-linked immunosorbent assay (ELISA) kit per manufacturer instructions (Sigma-Aldrich). Absorbance was measured at 450 nm using a VICTOR3 microplate reader (PerkinEimer, Inc., Waltham, MA, USA).

Mouse bile duct organoid culture. EHBD was isolated from adult mice and dissociated in Accutase (STEMCELL, Cambridge, MA, USA) at 37°C for 15 minutes, followed by filtration through a 70-µm strainer (BD Bioscience, San Jose, CA, USA) and centrifugation at 300 x *g* for 5 minutes. Cells were resuspended in Matrigel (Corning, Tewksbury, MA, USA) and plated in prewarmed 12- or 24-well plates, followed by overlying with 300 or 600 µL culture media (50% L-WRN [ATCC CRL-3276] conditioned media,[33] 1X penicillin-streptomycin, 1X GlutaMAX, 10 mM HEPES, 1X Fungizone, 1X gentamicin, 1X B27, and 1X N2 [Thermo Fisher Scientific] in advanced DMEM/F12 [Invitrogen]). Fibroblast growth factor 10 (100 ng/mL; PeproTech, Rocky Hill, NJ, USA) and epithelial growth factor (50 ng/mL; Invitrogen) were added to the culture media for the first 3 days. Bile duct organoids (BDOs) were passaged every 7 to 10 days by mechanically dissociating organoids with a 25-gauge needle and resuspending in Matrigel at 1:3 to 1:4 ratios. BDO growth and proliferation were measured after administration of recombinant IL-33 (100 ng/mL; R&D Systems) or nuclear factor-κB (NF-κB) inhibitor N4-[2-(4-phenoxyphenyl)ethyl]-4,6-quinazolinediamine (QNZ; 1 µM, pretreatment for 1 hour; Cayman Chemical, Ann Arbor, MI, USA).

Quantitative real-time polymerase chain reaction. EHBD was isolated and placed into RNA*later* (Qiagen, Hilden, Germany). Tissue was transferred to RPE buffer (RNeasy Micro Kit, Qiagen) and homogenized using a bead mill homogenizer (VWR, Radnor, PA, USA). Total RNA was isolated from whole EHBD tissue or organoids after DNase I digestion (Qiagen) using an RNeasy Mini Kit or RNeasy Micro Kit (Qiagen). Complementary DNA (cDNA) was generated from 500 ng total RNA using the iScript cDNA synthesis kit (Bio-Rad, Hercules, CA, USA). Quantitative real-time polymerase chain reaction (qPCR) was performed in duplicate reactions of 20 µL total volume using 100 µM of forward and reverse primers (Table 2), 1 µL SYBR Green I Nucleic Acid Stain (Lonza, Rockland, ME, USA), and 0.1 µL Platinum Taq DNA polymerase (Invitrogen; Carlsbad, CA, USA) using a CFX96 Real-Time thermocycler (Bio-Rad, C1000; Hercules, CA, USA). Target gene expression was normalized to *Hprt* control mRNA abundance.

Cell lines. The L-WRN (CRL-3276) cell line[33] was purchased from ATCC (Manassas, VA, USA) on November 6, 2015. The third and fourth passages were used to generate conditioned media for organoid culture. The mycoplasma detection test (ATCC) was performed on all cultures before experiments (last check on May 18, 2018).

Organoid proliferation. BDOs were incubated in 5-ethynyl-2′-deoxyuridine (EdU) (10 µM for 9 hours; Thermo Fisher Scientific), washed with PBS, and fixed with 4% PFA for 10 minutes at RT. After washing with PBS and permeabilization with 0.5% PBS-Triton X-100 for 20 minutes, BDOs were incubated in the EdU reaction cocktail from a Click-iT Plus EdU kit (Thermo Fisher Scientific). BDOs were then washed, resuspended in ice-cold PBS, placed on a slide, and mounted with ProLong Gold with DAPI (Life Technologies). A Nikon Eclipse E800 microscope (Nikon, Tokyo, Japan) was used to take images.

Statistical analysis. GraphPad Prism 7 (La Jolla, CA, USA) was used for one-way analysis of variance (ANOVA) and unpaired Student *t* test statistical analyses. Quantitative values were expressed as actual numbers (mRNA expression, serum SHH expression, BD thickness, or area) and compared with the baseline (wild-type [WT] animal or vehicle) where applicable. Significance was set at $P < 0.05$. Results were presented as mean +/- standard error of mean.

RESULTS

HH signals to stromal cells in EHBDs. We examined the cellular basis for HH signaling in EHBD (Fig. 1A) to identify HH-responsive cells expressing the general HH pathway components.[34, 35] Using *Gli1$^{lacZ/+}$, Gli2$^{lacZ/+}$*, *Gli3$^{lacZ/+}$*, and *Ptch$^{lacZ/+}$* reporter mice, we identified putative sites of active HH response in mouse EHBDs (i.e., *Gli1*-expressing and *Ptch1*-expressing cells) as well as those sites that are competent to transduce HH signals through expression of the GLI transcriptional effectors (i.e., *Gli*-expressing cells). As expected, WT mice lacked β-galactosidase activity (Fig. 1B). HH target gene expression was observed in stromal cells in *Gli1$^{lacZ/+}$* and *Ptch$^{lacZ/+}$* mice (Fig. 1C,F); similar stromal expression was noted in *Gli2$^{lacZ/+}$* and *Gli3$^{lacZ/+}$* mice (Fig. 1D,E). We tested WT mouse EHBDs for mRNA abundance of the HH ligands *Shh* and *Ihh*. Although mouse EHBDs lacked detectable *Shh* expression at baseline, they readily expressed *Ihh* mRNA (Fig. 1G). These findings indicate that EHBD stromal cells are HH-signaling cells, and IHH is the dominant HH ligand in EHBDs.

***pCMV-Shh* and *Gli1$^{lacZ/lacZ}$* mice model chronic HH ligand overexpression and Gli1 inhibition in EHBDs.** We previously reported the use of genetically engineered murine models of HH ligand overexpression (*pCMV-Shh*) and the loss of the transcriptional activator *Gli1* (*Gli $^{lacZ/lacZ}$*) to investigate the consequences of modulating HH signaling on *Helicobacter pylori*–induced stomach metaplasia.[2, 4] We took advantage of these mouse models to examine the contribution of HH signaling in mouse EHBDs. We identified the site of HH ligands and effector *Gli1* expression in EHBDs of *pCMV-Shh* mice by *in situ* hybridization (Fig. 2B-D). EHBDs from WT mice did not express *Shh* mRNA (Fig. 2A), consistent with the absence of detectable *Shh* mRNA expression in WT mouse EHBDs by qPCR (Fig. 1G). In *pCMV-Shh* mice, *Shh* mRNA and *Ihh* mRNA were expressed and localized in epithelial cells (Fig. 2B,C). Consistent with findings in *Gli1$^{lacZ/+}$* mice, *Gli1* mRNA was localized in stromal cells in EHBDs of *pCMV-Shh* (Fig. 2D). Additionally, GLI1 was stromal in *pCMV-Shh; Gli1$^{lacZ,/+}$* and *pCMV-Shh; Gli1$^{lacZ./lacZ}$* mice (Fig. 2E,F). Further, *pCMV-Shh* mice had an increased level of circulating SHH ligand in serum compared with WT and *Gli1$^{lacZ/lacZ}$* mice (Fig. 2G). *Gli1, Gli2,* and *Ptch1* mRNA abundance in *pCMV-Shh* mice, compared with WT and *Gli1$^{lacZ/lacZ}$* mice, was significantly increased (Fig. 2H-J). Thus, we used the *pCMV-Shh* mouse model to study the consequences of

increased chronic HH pathway activity, and *Gli1*^{lacZ/lacZ} mice to study decreased canonical HH pathway activity in EHBD stroma *in vivo*.

***HH overexpression amplifies IL-33–induced epithelial cell proliferation in vivo*.** In chronic progressive fibroproliferative disorders, such as primary sclerosing cholangitis, chronic injury is associated with up-regulation of inflammatory cytokines.[36] Cholangiocarcinoma, which frequently complicates cholangiopathies, is associated with upregulation of HH signaling and also cytokines IL-33 and IL-6.[7, 22, 25] Thus, we examined human EHBD cholangiocarcinoma and adjacent non-cancerous tissue for expression of inflammatory cytokines with immunohistochemistry. We demonstrated that IL-33, which is an alarmin and potent biliary mitogen,[15, 21] was expressed in non-cancerous EHBD and was overexpressed in cholangiocarcinoma (Fig. 3A). Further, normal adjacent bile duct and EHBD cholangiocarcinoma cells strongly expressed the IL-6R receptor (IL-6) (Fig. 3B).

We tested the HH mouse models to determine whether increased HH signaling synergizes with inflammatory cytokines to promote cell proliferation. We showed that mouse EHBDs express the IL-33 receptor ST2, which is primarily localized in epithelial cells at baseline and in both epithelial and stromal cells after IL-33 treatment (Fig. 4A). We treated the *pCMV-Shh* and *Gli1*^{lacZ/lacZ} mouse models with IL-33 (Fig. 4B, schema). We examined EHBDs of WT, *pCMV-Shh*, and *Gli1*^{lacZ/lacZ} mice macroscopically and histologically and observed no gross morphological differences between IL-33 and vehicle-treated mice (Fig. 4C,D, upper panels). However, BD thickness, an indicator of hyperplasia, was increased in IL-33–treated *pCMV-Shh* mice compared with WT controls and *Gli1*^{lacZ/lacZ} mice (Fig. 4E), with increased cellularity observed by H&E staining (Fig. 4D).

Analysis of BrdU incorporation demonstrated no difference in epithelial and stromal cell proliferation in EHBDs of WT, *pCMV-Shh*, and *Gli1*^{lacZ/lacZ} vehicle-treated mice (Fig. 5A, upper panel; quantified in B). As expected, proliferation was very low because cholangiocytes are virtually mitotically dormant at baseline.[5] IL-33 induced proliferation of both epithelial and stromal cells (Fig. 5A-C). However, HH overexpression amplified the proliferative effect of IL-33 on epithelial cells, but not on stromal cells (Fig. 5A-C). Further, *Gli1* ablation blunted the IL-

33–induced epithelial cell proliferation (Fig. 5A,B). The results suggest that IL-33 is the primary driver of EHBD cell proliferation and HH signaling enhances cytokine-induced epithelial cell proliferation.

IL-6 increase is associated with HH and IL-33 synergism. Both HH and IL-33 signaling are associated with IL-6 upregulation in human cholangiopathies. Therefore, we hypothesized that IL-6 may contribute to the synergistic effect of HH and IL-33 signaling on biliary proliferation in EHBDs. We demonstrated that IL-33 increases IL-6R expression in epithelial and stromal cells in WT mouse EHBDs (Fig. 6A). Although WT and *pCMV-Shh* mice exhibited similar increase in *Il6* mRNA expression after IL-33 treatment, *Gli1* ablation blunted the *Il6* mRNA response to IL-33^{lacZlacZ} (Fig. 6B). These findings suggested that HH signaling is important for IL-33-induced *Il6* expression.

We next examined the effect of IL-33 on expression of HH components by immunohistochemistry and qPCR. We demonstrated that after treatment with IL-33, *Gli1* expression remained stromal (Supporting Fig. S1A-C). We further showed, that mRNA abundance of HH components was not significantly changed in various IL-33-treated mouse strains (Supporting Fig. S1D-H). In particular, *Shh* mRNA still was not expressed in WT and *Gli1$^{lacZ/lacZ}$* mice even after IL-33 treatment (Supporting Fig. S1D). While *Gli1* mRNA expression remained undetectable in *Gli1$^{lacZ/lacZ}$* mice treated with IL-33 (Supporting Fig. S1F). Collectively, these data indicated that IL-33 does not have a direct effect on HH signaling modulator expression. However, HH signaling, and specifically GLI1, primes EHBD for the proliferative response to IL-33.

IL-33 induces epithelial cell proliferation in vitro. To study the direct effect of IL-33 and HH on biliary cell proliferation, we examined WT mice–derived BDOs. We examined organoids for mRNA abundance of *St2* and the HH signaling effector *Gli1*. As expected from the mouse tissue expression patterns (cf. Fig. 1), BDOs expressed *St2* but lacked *Gli1* mRNA expression (Fig. 7A). Thus, BDOs, which are comprised of only epithelial cells, do not exhibit canonical GLI1-mediated HH signaling. We investigated the effect of IL-33 on epithelial cell proliferation in BDOs. Consistent with our *in vivo* data, we found that IL-33 stimulated increased BDO growth

(Fig. 7B,C) through increased epithelial cell proliferation, as measured by EdU incorporation (Fig. 7D,E). Further, there was no difference in the IL-33-inducedproliferative response between WT, *pCMV-Shh*, and *Gli1*$^{lacZ/lacZ}$ mice-derived organoids (Fig. S2A,B). This result is consistent with the *in vivo* observation that HH signaling occurs in stromal cells.

To identify the potential mechanism of IL-33-induced BDO proliferation, we used the NF-κB inhibitor, QNZ,[37] as IL-33 has been previously reported to signal through NF-κB.[38] Pre-treatment of BDOs with QNZ effectively prevented IL-33 induced BDO proliferation (Fig. 7D,E). Together, our findings suggest that IL-33 can directly stimulate epithelial proliferation in an NF-κB-dependent manner, and that the HH pathway indirectly supports IL-33–driven epithelial proliferation through activation of signaling in stromal cells.

DISCUSSION

Our current results demonstrate that EHBD stromal cells express the HH transcriptional effectors GLI1, GLI2, and GLI3, as well as the receptor PTCH1, and thus appear to be the primary cells responding to HH ligand. They also demonstrated that HH ligand expression is limited to the epithelium, and that IHH is the predominant HH ligand expressed both under basal conditions and after inflammatory challenge with IL-33. We used *pCMV-Shh* mice as a model to study the consequences of HH ligand overexpression in EHBDs because IHH and SHH both signal through the same receptor and GLI effectors. [39] Although the CMV promoter expressing the *Shh* transgene should be non-specific, it has been demonstrated to preferentially drive expression in certain cells within different organ systems.[40] For example, in the stomach, expression of SHH in *pCMV-Shh* mice was enriched in gastric chief cells.[2] In our genetically engineered mouse model of HH ligand overexpression, *Shh* and *Ihh* were localized to epithelial cells. Therefore, our observation of HH ligand expression in epithelial cells and GLI1 in stromal cells is consistent with HH signaling from epithelial to stromal cells, as observed in other organ systems, including the stomach and intestine.[2, 41, 42]

Our studies further suggest that increased HH signaling alone is insufficient to induce EHBD epithelial cell proliferation. However, HH overexpression augmented the proliferative effect of the inflammatory cytokine and alarmin IL-33 on EHBD epithelial cells, but not stromal cells.

Interestingly, reduction in canonical HH signaling in receptive stromal cells attenuated the IL-33 effect on epithelial proliferation, indicative that synergism between HH and IL-33 signaling involves GLI1-positive stromal cells. These findings suggest that BECs respond to HH upregulation differentially with no changes in cell proliferation at basal conditions and with an enhanced proliferative response under inflammatory challenge. However, the HH-dependent factor that enhances epithelial cell response to IL-33 is unknown.

As both HH and IL-33 pathways are reported to signal through IL-6,[23, 43, 44] we explored the potential role of interleukin 6 (IL-6) in the synergism between HH and IL-33 signaling in IL-33-induced cell proliferation in EHBDs. We demonstrated that IL-33 and IL-6 receptor IL-6R are expressed in human cholangiocarcinoma and adjacent normal EHBD tissue. We also demonstrated that IL-33 induces expression of *Il6*, which is in part dependent on GLI1-positive stromal cells. Therefore, GLI1-expressing stromal cells might be important in epithelial cell responses to inflammatory cytokines. It is possible that HH ligand overexpression "primes" GLI1-positive stromal cells and activates GLI1 gene targets, which indirectly affects cytokine signaling in EHBD epithelial cells. Alternatively, IL-33 signaling "primes" the epithelial cells to be more responsive to HH-dependent stroma-derived factors (Fig. 8).

It was reported that IL-33 promotes cholangiocyte proliferation indirectly through type 2 innate lymphoid cell IL-13.[15] However, in our biliary organoid culture, we demonstrated that IL-33 also can directly induce proliferation in biliary progenitor cells. This IL-33 proliferative effect on biliary progenitor cells is NF-κB-dependent. The latter observation is interesting, as IL-33 induces cytokine expression via NF-κB.[44] In addition, NF-κB activation in cholangiocytes exposed to liver fluke *Opisthorchis viverrini* is associated with upregulation of IL-6 and IL-8,[45] and IL-33 overexpression occurs in hepatobiliary parasitic infection clonorchiasis[17] and visceral leishmaniasis.[18] Thus, IL-33 can affect EHBD responses both directly and indirectly through regulating another cytokine function.

These data have relevance to human diseases, as IL-6 overexpression was recently described in cholangiocarcinomas arising in patients with primary sclerosing cholangitis associated with extensive PBG hyperplasia.[26] HH signaling upregulation was also reported in patients with primary sclerosing cholangitis and PBG hyperplasia.[13] An association between IL-33 and IL-6

has been shown in patients with cholangiocarcinoma, where IL-33 overexpression was observed in cancer involving large versus small bile ducts, and was associated with IL-6 overexpression.[25]

In summary, we report a previously unknown role for HH signaling in the regulation of EHBD homeostasis by promoting context-dependent BEC proliferation contributing to EHBD hyperplasia. This involves crosstalk between HH ligand-producing cells and receptive GLI1-positive stromal cells (Fig. 8). We also showed that the alarmin IL-33 can directly induce epithelial cell proliferation. Future studies identifying the proliferative signals from HH-responding GLI1-positive stromal cells toward epithelial cells and the mechanisms of HH signaling and inflammatory cytokine interactions will be needed. They could provide insight into how and, importantly, when HH and/or cytokine signaling can be targeted to prevent EHBD hyperplasia, which can be preneoplastic in chronic biliary conditions, such as primary sclerosing cholangitis.

REFERENCES

1)   Robbins DJ, Fei DL, Riobo NA. The Hedgehog signal transduction network. Sci Signal 2012;5:re6.

2)   El-Zaatari M, Kao JY, Tessier A, Bai L, Hayes MM, Fontaine C, et al. Gli1 deletion prevents Helicobacter-induced gastric metaplasia and expansion of myeloid cell subsets. PLoS One 2013;8:e58935.

3)   Armas-Lopez L, Zuniga J, Arrieta O, Avila-Moreno F. The Hedgehog-GLI pathway in embryonic development and cancer: implications for pulmonary oncology therapy. Oncotarget 2017;8:60684-60703.

4)   Ding L, Hayes MM, Photenhauer A, Eaton KA, Li Q, Ocadiz-Ruiz R, et al. Schlafen 4-expressing myeloid-derived suppressor cells are induced during murine gastric metaplasia. J Clin Invest 2016;126:2867-2880.

5)   Omenetti A, Diehl AM. Hedgehog signaling in cholangiocytes. Curr Opin Gastroenterol 2011;27:268-275.

6)   Maroni L, Haibo B, Ray D, Zhou T, Wan Y, Meng F, et al. Functional and structural features of cholangiocytes in health and disease. Cell Mol Gastroenterol Hepatol 2015;1:368-380.

7)   Razumilava N, Bronk SF, Smoot RL, Fingas CD, Werneburg NW, Roberts LR, et al. miR-25 targets TNF-related apoptosis inducing ligand (TRAIL) death receptor-4 and promotes apoptosis resistance in cholangiocarcinoma. Hepatology 2012;55:465-475.

8)   Razumilava N, Gradilone SA, Smoot RL, Mertens JC, Bronk SF, Sirica AE, et al. Non-canonical Hedgehog signaling contributes to chemotaxis in cholangiocarcinoma. J Hepatol 2014;60:599-605.

9)   Lazaridis KN, LaRusso NF. The cholangiopathies. Mayo Clin Proc 2015;90:791-800.

10)   DiPaola F, Shivakumar P, Pfister J, Walters S, Sabla G, Bezerra JA. Identification of intramural epithelial networks linked to peribiliary glands that express progenitor cell markers and proliferate after injury in mice. Hepatology 2013;58:1486-1496.

11)   Carpino G, Renzi A, Franchitto A, Cardinale V, Onori P, Reid L, et al. Stem/progenitor cell niches involved in hepatic and biliary regeneration. Stem Cells Int 2016;2016:3658013.

12)   Terada T, Nakanuma Y. Pathologic observations of intrahepatic peribiliary glands in 1,000 consecutive autopsy livers: IV. Hyperplasia of intramural and extramural glands. Hum Pathol 1992;23:483-490.

13)   Carpino G, Cardinale V, Renzi A, Hov JR, Berloco PB, Rossi M, et al. Activation of biliary tree stem cells within peribiliary glands in primary sclerosing cholangitis. J Hepatol 2015;63:1220-1228.

14)   Patman G. Biliary tract. IL-33, innate lymphoid cells and IL-13 are required for cholangiocyte proliferation. Nat Rev Gastroenterol Hepatol 2014;11:456.

15)   Li J, Razumilava N, Gores GJ, Walters S, Mizuochi T, Mourya R, et al. Biliary repair and carcinogenesis are mediated by IL-33-dependent cholangiocyte proliferation. J Clin Invest 2014;124:3241-3251.

16)   Baier JL, Mattner J. Mechanisms of autoimmune liver disease. Discov Med 2014;18:255-263.

17)   Yu Q, Li XY, Cheng XD, Shen LP, Fang F, Zhang B, et al. Expression and potential roles of IL-33/ST2 in the immune regulation during Clonorchis sinensis infection. Parasitol Res 2016;115:2299-2305.

18)   Rostan O, Gangneux JP, Piquet-Pellorce C, Manuel C, McKenzie AN, Guiguen C, et al. The IL-33/ST2 axis is associated with human visceral leishmaniasis and suppresses Th1

responses in the livers of BALB/c mice infected with Leishmania donovani. MBio 2013;4:e00383-00313.

19) Huan SL, Zhao JG, Wang ZL, Gao S, Wang K. Relevance of serum interleukin-33 and ST2 levels and the natural course of chronic hepatitis B virus infection. BMC Infect Dis 2016;16:200.

20) Wang J, Zhao P, Guo H, Sun X, Jiang Z, Xu L, et al. Serum IL-33 levels are associated with liver damage in patients with chronic hepatitis C. Mediators Inflamm 2012;2012:819636.

21) Nakagawa H, Suzuki N, Hirata Y, Hikiba Y, Hayakawa Y, Kinoshita H, et al. Biliary epithelial injury-induced regenerative response by IL-33 promotes cholangiocarcinogenesis from peribiliary glands. Proc Natl Acad Sci U S A 2017;114:E3806-E3815.

22) Yamada D, Rizvi S, Razumilava N, Bronk SF, Davila JI, Champion MD, et al. IL-33 facilitates oncogene-induced cholangiocarcinoma in mice by an interleukin-6-sensitive mechanism. Hepatology 2015;61:1627-1642.

23) Mathew E, Collins MA, Fernandez-Barrena MG, Holtz AM, Yan W, Hogan JO, et al. The transcription factor GLI1 modulates the inflammatory response during pancreatic tissue remodeling. J Biol Chem 2014;289:27727-27743.

24) Pereira TA, Xie G, Choi SS, Syn WK, Voieta I, Lu J, et al. Macrophage-derived Hedgehog ligands promotes fibrogenic and angiogenic responses in human schistosomiasis mansoni. Liver Int 2013;33:149-161.

25) Sawada R, Ku Y, Akita M, Otani K, Fujikura K, Itoh T, et al. Interleukin-33 overexpression reflects less aggressive tumour features in large-duct type cholangiocarcinomas. Histopathology 2018;73:259-272.

26) Carpino G, Cardinale V, Folseraas T, Overi D, Grzyb K, Costantini D, et al. Neoplastic transformation of peribiliary stem cell niche in cholangiocarcinoma arisen in primary sclerosing cholangitis. Hepatology 2018.

27) Ahn S, Joyner AL. Dynamic changes in the response of cells to positive hedgehog signaling during mouse limb patterning. Cell 2004;118:505-516.

28) Bai CB, Auerbach W, Lee JS, Stephen D, Joyner AL. Gli2, but not Gli1, is required for initial Shh signaling and ectopic activation of the Shh pathway. Development 2002;129:4753-4761.

29) Goodrich LV, Milenkovic L, Higgins KM, Scott MP. Altered neural cell fates and medulloblastoma in mouse patched mutants. Science 1997;277:1109-1113.

30) Harfe BD, Scherz PJ, Nissim S, Tian H, McMahon AP, Tabin CJ. Evidence for an expansion-based temporal Shh gradient in specifying vertebrate digit identities. Cell 2004;118:517-528.

31) Bai CB, Joyner AL. Gli1 can rescue the in vivo function of Gli2. Development 2001;128:5161-5172.

32) Garcia AD, Petrova R, Eng L, Joyner AL. Sonic hedgehog regulates discrete populations of astrocytes in the adult mouse forebrain. J Neurosci 2010;30:13597-13608.

33) Miyoshi H, Stappenbeck TS. In vitro expansion and genetic modification of gastrointestinal stem cells in spheroid culture. Nat Protoc 2013;8:2471-2482.

34) Agren M, Kogerman P, Kleman MI, Wessling M, Toftgard R. Expression of the PTCH1 tumor suppressor gene is regulated by alternative promoters and a single functional Gli-binding site. Gene 2004;330:101-114.

35) Dai P, Akimaru H, Tanaka Y, Maekawa T, Nakafuku M, Ishii S. Sonic Hedgehog-induced activation of the Gli1 promoter is mediated by GLI3. J Biol Chem 1999;274:8143-8152.

36) Razumilava N, Gores GJ, Lindor KD. Cancer surveillance in patients with primary sclerosing cholangitis. Hepatology 2011;54:1842-1852.

37) Tobe M, Isobe Y, Tomizawa H, Nagasaki T, Takahashi H, Fukazawa T, et al. Discovery of quinazolines as a novel structural class of potent inhibitors of NF-kappa B activation. Bioorg Med Chem 2003;11:383-391.

38) Lin J, Zhang L, Zhao G, Su Z, Deng R, Pflugfelder SC, et al. A novel interleukin 33/ST2 signaling regulates inflammatory response in human corneal epithelium. PLoS One 2013;8:e60963.

39) Varjosalo M, Taipale J. Hedgehog: functions and mechanisms. Genes Dev 2008;22:2454-2472.

40) Schmidt EV, Christoph G, Zeller R, Leder P. The cytomegalovirus enhancer: A pan-active control element in transgenic mice. Mol Cell Biol 1990;10:4406-4411.

41) Razumilava N, Gumucio DL, Samuelson LC, Shah YM, Nusrat A, Merchant JL. Indian Hedgehog Suppresses Intestinal Inflammation. Cell Mol Gastroenterol Hepatol 2018;5:63-64.

42)   Westendorp BF, Buller N, Karpus ON, van Dop WA, Koster J, Versteeg R, et al. Indian Hedgehog Suppresses a Stromal Cell-Driven Intestinal Immune Response. Cell Mol Gastroenterol Hepatol 2018;5:67-82 e61.

43)   Hirsova P, Ibrahim SH, Bronk SF, Yagita H, Gores GJ. Vismodegib suppresses TRAIL-mediated liver injury in a mouse model of nonalcoholic steatohepatitis. PLoS One 2013;8:e70599.

44)   Fattori V, Hohmann MSN, Rossaneis AC, Manchope MF, Alves-Filho JC, Cunha TM, et al. Targeting IL-33/ST2 signaling: regulation of immune function and analgesia. Expert Opin Ther Targets 2017;21:1141-1152.

45)   Ninlawan K, O'Hara SP, Splinter PL, Yongvanit P, Kaewkes S, Surapaitoon A, et al. Opisthorchis viverrini excretory/secretory products induce toll-like receptor 4 upregulation and production of interleukin 6 and 8 in cholangiocyte. Parasitol Int 2010;59:616-621.

TABLES:

Table 1. Antibody list. IgG – immunoglobulin.

Table 2. Primer list. bp – base pair.

FIGURE LEGENDS

FIG. 1. The HH signaling receptive cells are located in the EHBD stroma. Mouse EHBDs were isolated from wild-type (WT) and reporter *Gli1$^{lacZ/+}$, Gli2$^{lacZ/+}$, Gli3$^{lacZ/+}$*, and *Ptch1$^{lacZ/+}$* mice and stained by H&E (A) and for β-galactosidase activity (X-gal) (B-F). The BD lumen was marked with the asterisks, epithelial cells with arrows, and stromal cells with arrowheads. Scale bars: 50 μm (representative images of 2-5 samples per genotype). Total RNA was isolated from EHBDs of WT mice and analyzed for mRNA expression by qPCR of *Shh* and *Ihh* referenced to *Hprt* (G) (n = 15-16 animals per group). Results are expressed as the mean +/- SEM.

FIG. 2. *pCMV-Shh* and *Gli1$^{lacZ/lacZ}$* mice model chronic HH overexpression and inhibition in EHBDs.** EHBDs from wild-type (WT), *pCMV-Shh* and *Gli1$^{lacZ/lacZ}$* mice were studied for expression of HH ligands and signaling targets. We analyzed EHBDs from WT and *pCMV-Shh* mice with *in situ* hybridization (RNAscope) for expression of *Shh* mRNA (A and B) (arrows)

and EHBDs from *pCMV-Shh* mice for expression of *Ihh* mRNA (C) and *Gli1* mRNA (D) (representative images of two samples). *Gli1* expression was also studied by immunofluorescence for β-galactosidase (E and F, red) (arrows) in *pCMV-Shh*; *Gli1*^{lacZ/+} and *pCMV-Shh*; *Gli1*^{lacZ/lacZ} mice. Cell nuclei were marked with DAPI (blue) (representative images of one and two samples, respectively). The epithelial cells were marked by arrows, stromal cells were marked by arrowheads, and lumen by asterisks. Scale bars: 20 µm. The serum level of the SHH ligand was measured by ELISA in WT, *pCMV-Shh*, and *Gli1*^{lacZ/lacZ} mice (G). Total RNA was isolated from EHBDs of the WT, *pCMV-Shh*, and *Gli1*^{lacZ/lacZ} mice and analyzed for mRNA expression by qPCR of *Gli1* (H), *Gli2* (I), and *Ptch1* (J) referenced to *Hprt*. Results were expressed as the mean +/- SEM (G-J) (n = 8-19 animals per group; one-way ANOVA). $*P < 0.05$, $**P < 0.01$, $****P < 0.0001$, ns – not significant.

FIG. 3. Cytokines IL-33 and IL-6 are expressed in human EHBDs. Human extrahepatic cholangiocarcinoma and adjacent non-cancerous tissue were examined for expression of IL-33 (A) and IL-6 receptor (IL-6R) (B) by immunohistochemistry (arrows - epithelial cells, arrowheads - stromal cells). The BD lumen was marked with the asterisks. Scale bars: 100 µm.

FIG. 4. HH signaling synergizes with IL-33 in EHBD hyperplasia. EHBDs from wild-type (WT) mice treated with either vehicle or IL-33 (1 µg/mouse/day for 4 days; necropsy on day 5) were analyzed by immunohistochemistry for ST2 expression (A; representative images of three samples). EHBDs from WT, *pCMV-Shh*, and *Gli1*^{lacZ/lacZ} mice treated with either vehicle (Veh) or mitogen IL-33 intraperitoneally (B) (schema) were examined macroscopically (C) (representative photographs; ruler scale: 1 mm) and histologically with H&E (D) (scale bars: 20 µm). The BD lumen was marked with the asterisks. The BD wall thickness from immunohistochemistry images was measured using ImageJ software and compared between WT, *pCMV-Shh*, and *Gli1*^{lacZ/lacZ} mice treated with either vehicle or IL-33 (D) (n = 7-11 animals per group). Results are expressed as the mean +/- SEM; one-way ANOVA. $*P < 0.05$, $**P < 0.01$, $***P < 0.001$, $****P < 0.0001$, ns – not significant.

FIG. 5. HH signaling synergizes with IL-33 to promote biliary cell proliferation. EHBDs from the WT, *pCMV-Shh*, and *Gli1*^{lacZ/lacZ} mice treated with either vehicle (Veh) or IL-33 (1

µg/mouse/day for 4 days; necropsy on day 5) were analyzed with immunofluorescence for cell proliferation. Proliferating cells were labeled by BrdU incorporation (A) (50 mg/kg, intraperitoneally, 2 hours before necropsy) (red). Cell nuclei were marked with DAPI (A) (blue) and biliary epithelial cells with CK19 (A) (green; original magnification 400×). Proliferating cells were quantified in the epithelial (B) (arrows) and stromal (C) (arrowheads) cell compartments with ImageJ software (n = 5-6 animals per group; ≥ 5 high power fields/BD; >500 cells/animal). Results were expressed as the mean +/- SEM (B-E); one-way ANOVA. *$P < 0.05$, **$P < 0.01$, ****$P < 0.0001$, ns – not significant.

FIG. 6. IL-33-induced IL-6 expression in mouse EHBDs involves *Gli1*. EHBDs from wild-type (WT) mice were analyzed by immunohistochemistry for IL-6 receptor (IL-6R) (A) expression after treatment with either vehicle (Veh) or recombinant IL-33 intraperitoneally (representative images of two samples). The BD lumen was marked with the asterisks, epithelial cells with arrows, and stromal cells with arrowheads. Scale bars: 10 µm. Total RNA was isolated from BDs of the WT, *pCMV-Shh,* and *Gli1*$^{lacZ/lacZ}$ mice treated with either vehicle or IL-33 and analyzed for mRNA expression by qPCR of *Il6* (B) referenced to *Hprt*. Results were expressed as the mean +/- SEM (n = 5-8 animals per group; one-way ANOVA). *$P < 0.05$, ns – not significant.

FIG. 7. IL-33–induced BDO cell proliferation *in vitro*. Total RNA was isolated from the WT mouse–derived organoids and analyzed for mRNA expression of *St2* and *Gli1* (A) (n = 3 organoid lines). BDOs were treated with vehicle or recombinant IL-33 (100 ng/mL) for 72 hours (D3) starting 24 hours after passage of established BDOs and analyzed for growth (B,C) (n = 6 technical replicates per group). In a separate experiment, BDOs were treated with either vehicle or pre-treated for 1 hour with the NF-κB inhibitor QNZ (1 µM) and then treated with recombinant IL-33 (100 ng/mL) for 72 hours (D3) after passaging of established BDOs. BDOs were analyzed for proliferation (D,E) (n = 3 technical replicates per group). The organoids were incubated with EdU for 9 hours to label proliferating cells (D) (green) among all BDO cells (D) (cell nuclei, DAPI, blue) (D) (original magnification 600×). ImageJ software was used to enumerate proliferating cells (E). Results were expressed as the mean +/- SEM; one-way ANOVA (C,E). ***$P < 0.001$, ****$P < 0.0001$.

FIG. 8. Model of HH and IL-33 synergy in IL-33-induced EHBD epithelial cell proliferation. IHH is secreted by epithelial cells and activates GLI1-positive stromal cells. After EHBD injury, IL-33 signals to GLI1-positive stromal and epithelial cells through ST2 receptor. IL-33 signaling involves the transcriptional effector NF-κB in epithelial cells. IL-33 induces IL-6 expression, which can signal to both epithelial and stromal cells. Increased epithelial cell proliferation induced by IL-33 is partially HH-dependent through an yet uncharacterized stromal factor.

SUPPLEMENTAL FIGURE LEGENDS

FIG. S1. IL-33 does not directly modulate HH signaling in EHBD. EHBDs from $Gli1^{lacZ/+}$ (A), $Gli1^{lacZ/lacZ}$ (B), and $pCMV\text{-}Shh$; $Gli1^{lacZ/lacZ}$ (C) mice were analyzed for expression of β-galactosidase histologically (X-gal, blue, arrowheads) and with immunohistochemistry (β-gal, red, arrowheads) after intraperitoneal administration of recombinant IL-33 (representative images of 1-3 samples). Cell nuclei were marked with DAPI (C) (blue). Scale bars: 20 µm. Total RNA was isolated from EHBDs of the WT, $pCMV\text{-}Shh$, and $Gli1^{lacZ/lacZ}$ mice treated with either vehicle or IL-33 and analyzed for mRNA expression by qPCR of Shh (D), Ihh (E), $Gli1$ (F), $Gli2$ (G), and $Ptch1$ (H) referenced to $Hprt$. Results were expressed as the mean +/- SEM (n = 5-19 animals per group; one-way ANOVA). ns – not significant.

FIG. S2. Synergism between HH and IL-33 signaling was not observed in BDO culture. BDOs were generated from the WT, $pCMV\text{-}Shh$, and $Gli1^{lacZ/lacZ}$ mice and treated with either vehicle or recombinant IL-33 (100 ng/mL) for 72 hours (D3) starting 24 hours after passage of established BDOs (A). BDOs were analyzed for proliferation (A,B) (n = 3 technical replicates per group). The organoids were incubated with EdU for 9 hours to label proliferating cells (A) (green) among all BDO cells (cell nuclei, DAPI, blue) (A) (original magnification 600×). ImageJ software was used to enumerate proliferating cells (E). Results were expressed as the mean +/- SEM; one-way ANOVA (C,E). ns – not significant.

TABLE 1. Antibody List

Target	Primary Antibody	Secondary Antibody
ST2	Rabbit, 1:200, ProSci (3363)	Biotinylated donkey, ImmunoResearch (712-065-153)
BrdU	Sheep, 1:200, Abcam (AB2284)	Alexa Fluor 594-Streptavidin, Invitrogen (S11227)
CK19	Rabbit; 1:250, Abcam (AB53119)	Alexa Fluor 488-labeled donkey IgG (H+L), Invitrogen (A21206)
IL-6Rα	Rabbit; 1:200, Santa Cruz (SC661)	Biotinylated donkey, ImmunoResearch (712-065-153)
IL-33 (human)	Goat; 1:20, R&D Systems (AF3625)	Biotinylated donkey, Abcam (AB6884)

TABLE 2. Primer list

Gene	Accession Number	Primer Sequence	Product Size (base pairs)
Hprt	NM_013556	Forward 5′-AACTTGCGCTCATCTTAGGCTTTG-3′ Reverse 5′-AGGACCTCTCGAAGTGTTGGATAC-3′	173 bp
Shh	NM_009170	Forward 5′-TCATCACAGAGATGGCCAAG-3′ Reverse 5′-GGAACTCACCCCCAATTACA-3′	122 bp
Ihh	NM_010544	Forward 5′-TGACAGAGATGGCCAGTGAG-3′ Reverse 5′-AGAGCTCACCCCCAACTACA-3′	119 bp
Gli1	NM_010296	Forward 5′-TATGTCAGGGTCCCAGGGTTATG-3′ Reverse 5′-GAGCCCGCTTCTTAGTCAGTTTG-3′	110 bp

Gli2	NM_001081125	Forward 5′-CCATTATGACCCTCACTCTGTC-3′ Reverse 5′-GGGTGTGGAGAAAGTCGTATC-3′	102 bp
Ptch1	NM_008957	Forward 5′-CTGCTGTGGTGGTGGTATTC-3′ Reverse 5′-GGCTTGTGAAACAGCAGAAA-3′	120 bp
St2	NM_001025602	Forward 5′-ATTCAGGGGACCATCAAGTG-3′ Reverse 5′-CGTCTTGGAGGCTCTTTCTG-3′	117 bp
Il-6	NM_031168.2	Forward 5'-TTCCATCCAGTTGCCTTCTTGG-3' Reverse 5'-TTCTCATTTCCACGATTTCCCAG-3'	175 bp

Mouse EHBD

A *Shh* mRNA — WT

B *Shh* mRNA — pCMV-Shh

C *Ihh* mRNA — pCMV-Shh

D *Gli1* mRNA — pCMV-Shh

E GLI1 — pCMV-Shh; Gli1^lacZ/+ — DAPI / β-gal

F GLI1 — pCMV-Shh; Gli1^lacZ/lacZ — DAPI / β-gal

G SHH serum level

H *Gli1* mRNA

I *Gli2* mRNA

J *Ptch1* mRNA
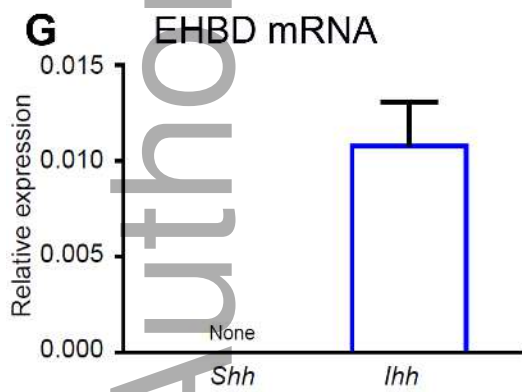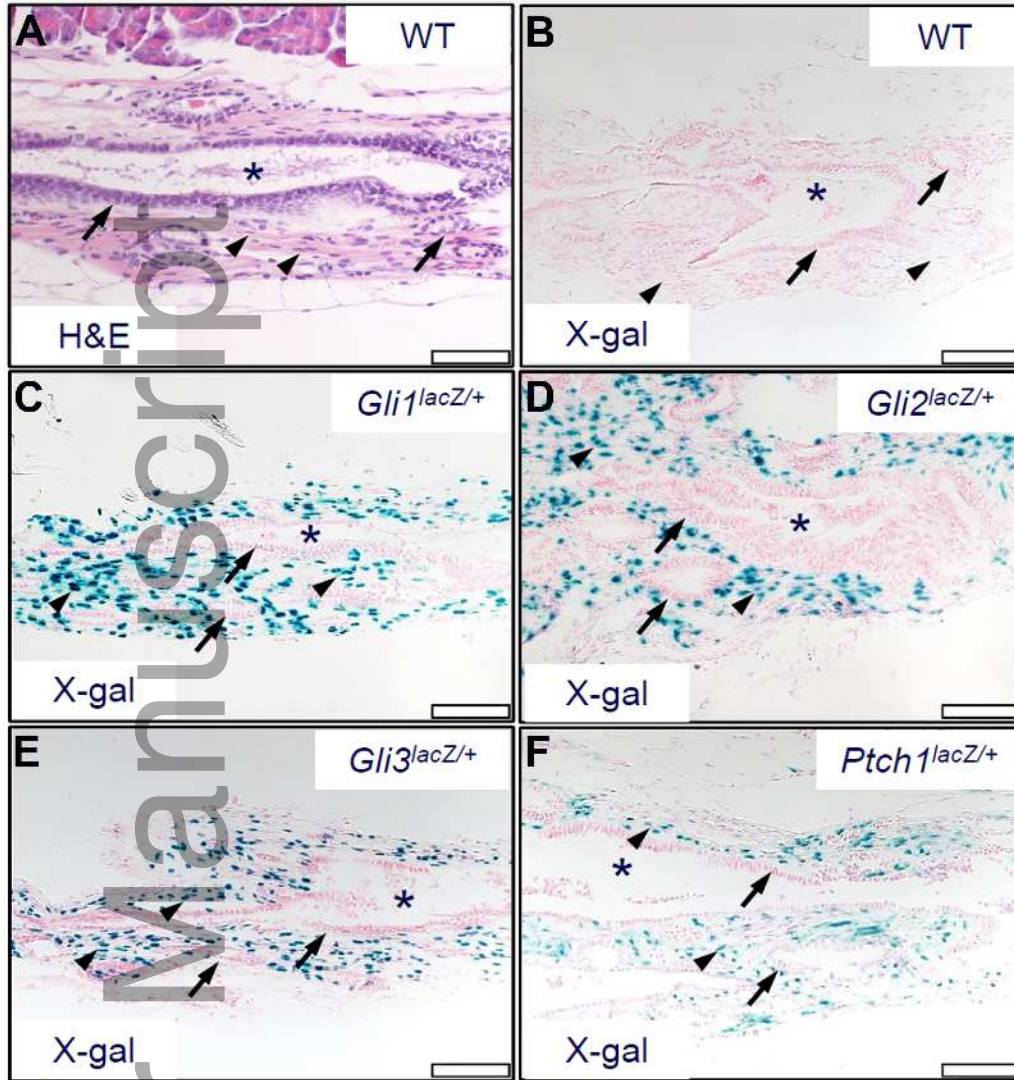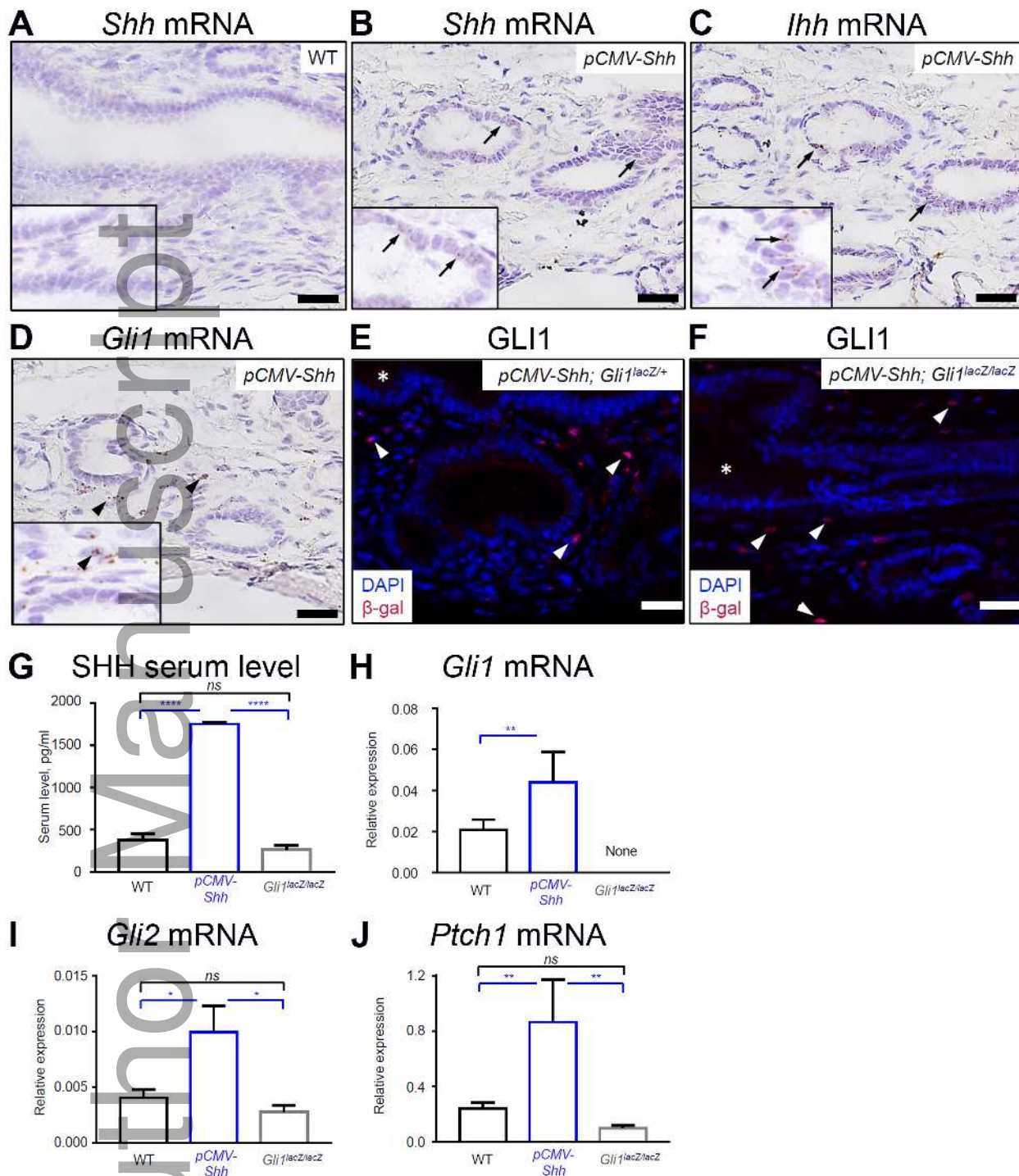
hep4_1295_f2.tif

Human EHBD

A IL-33

Non-cancerous Cholangiocarcinoma

B IL-6R

Non-cancerous Cholangiocarcinoma
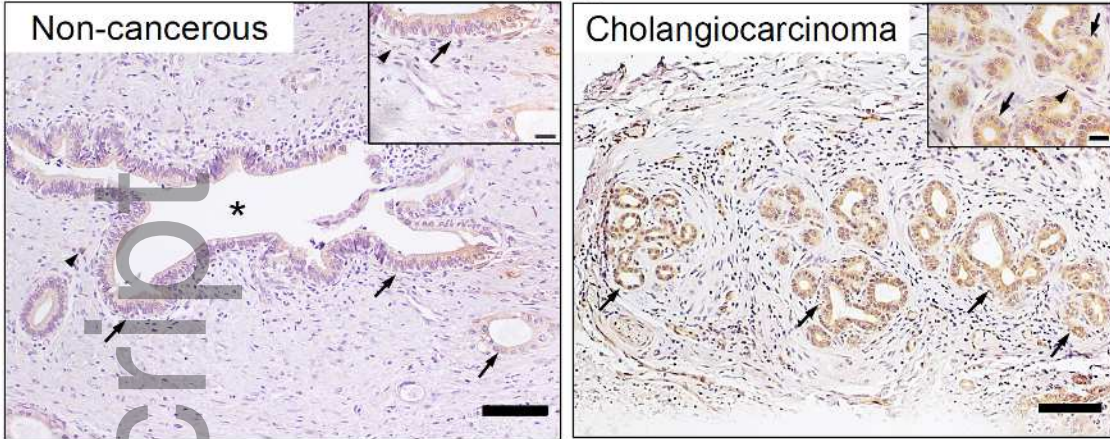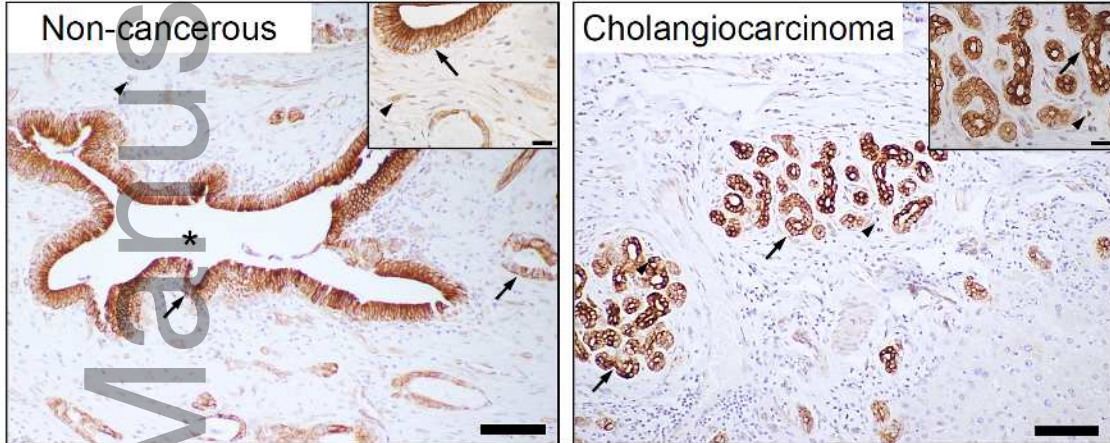
hep4_1295_f3.tif

A ST2 in WT EHBD

B

IL-33: 1µg i.p./mouse/day X 4 days
Necropsy: Day 5

C Mouse EHBDs

D Mouse EHBD

E BD thickness

hep4_1295_f4.tif

A

BrdU incorporation

DAPI BrdU CK19
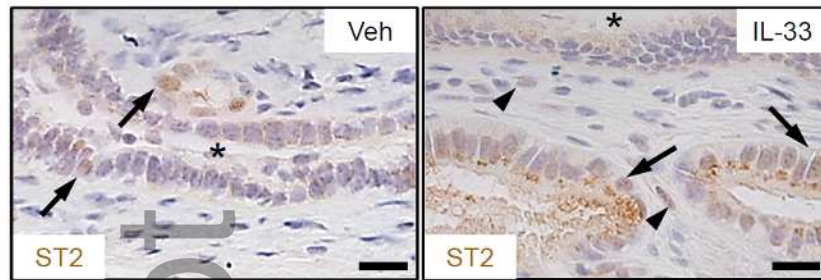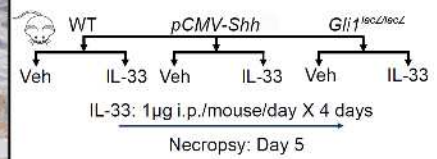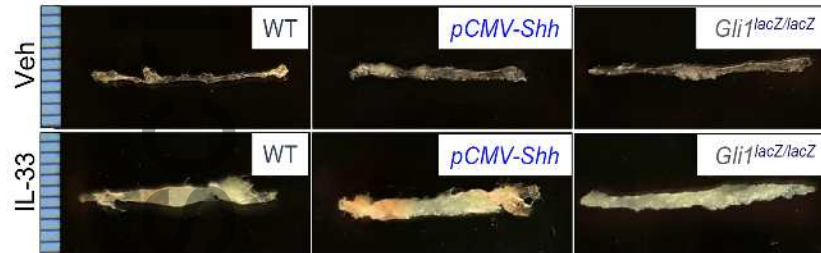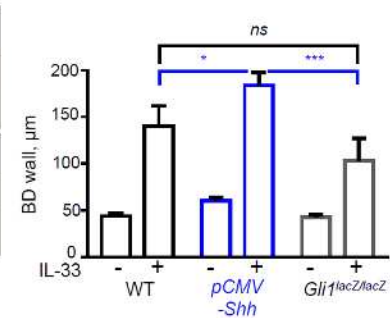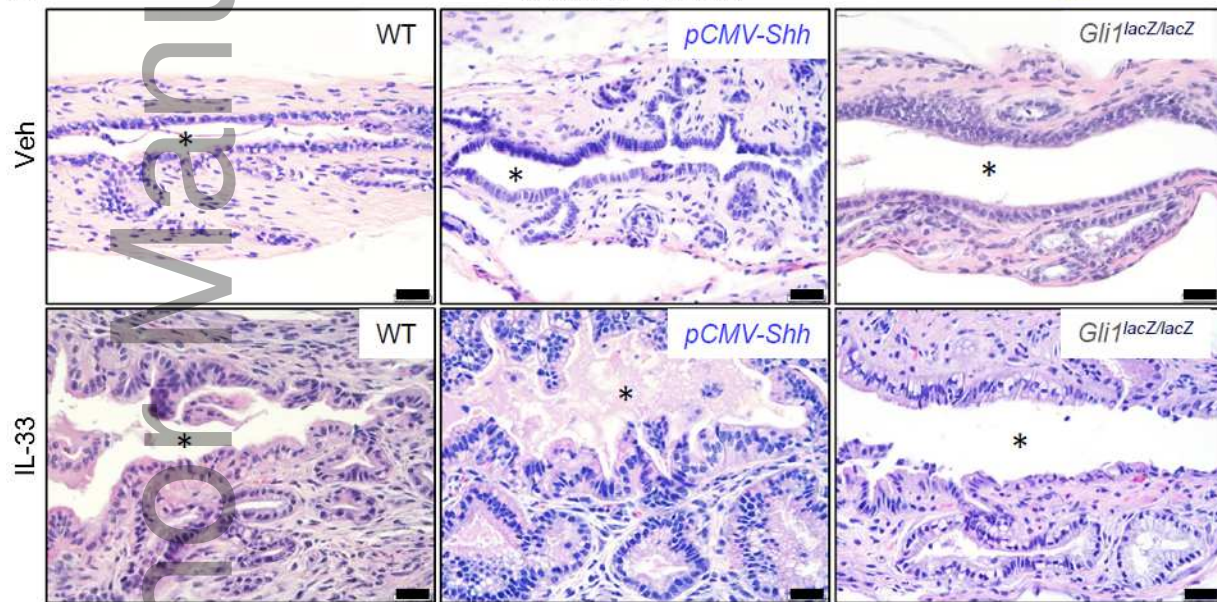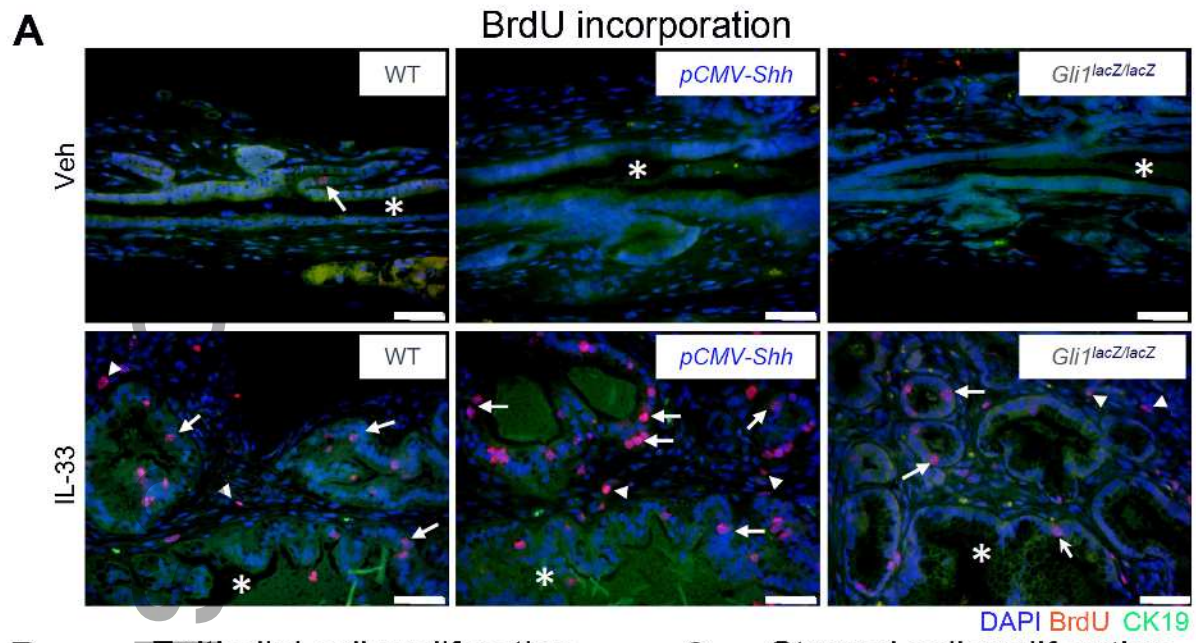
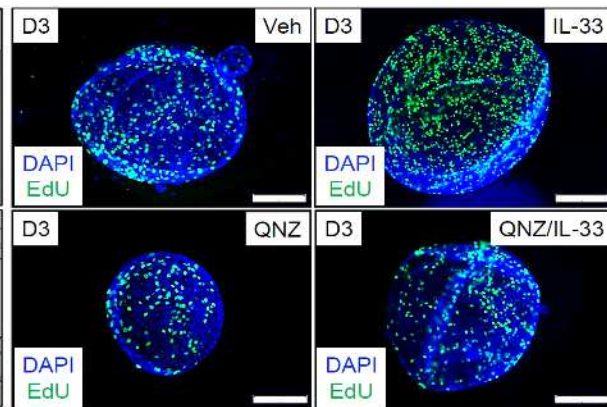# B
Epithelial cell proliferation
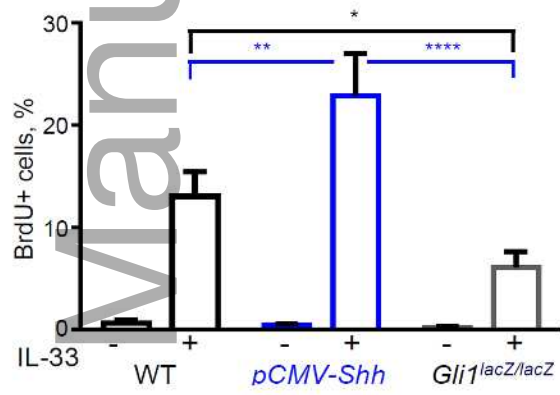
C
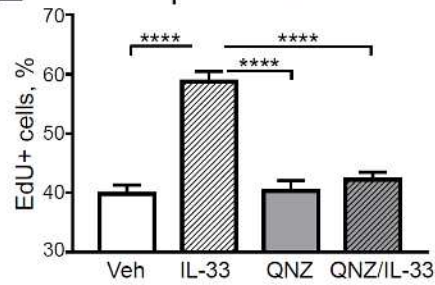## Stromal cell proliferation
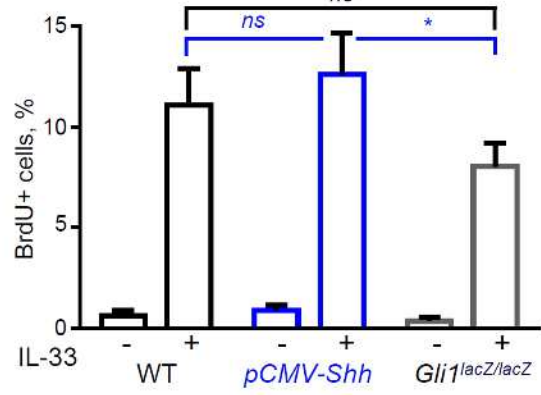
hep4_1295_f5.tif

A WT mouse EHBD
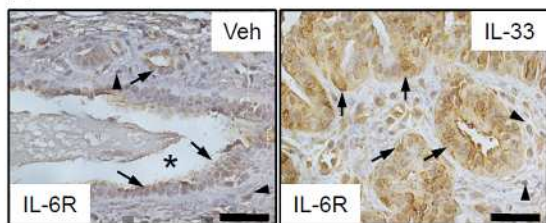
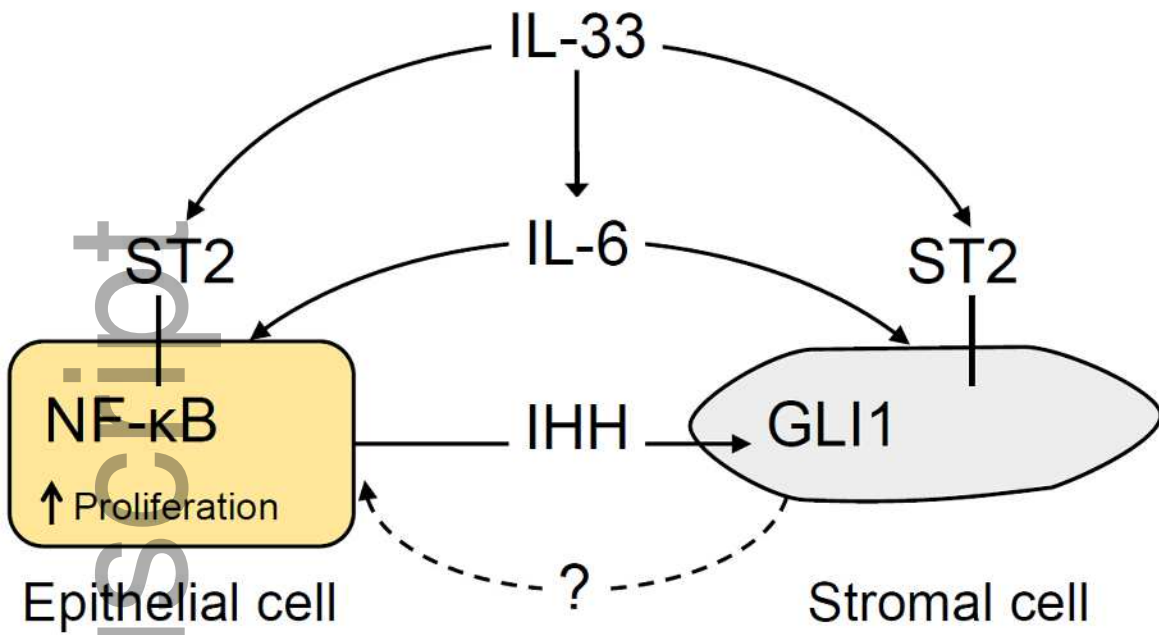**B** *Il6* mRNA
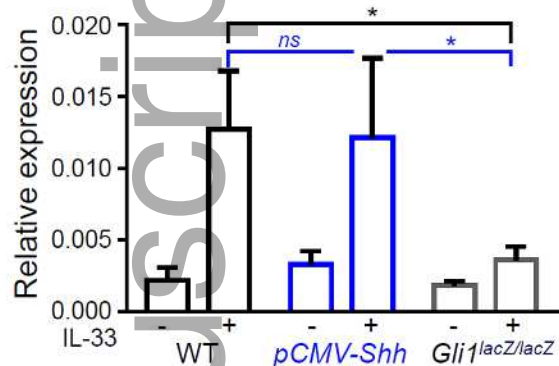
hep4_1295_f6.tif

A BDO mRNA
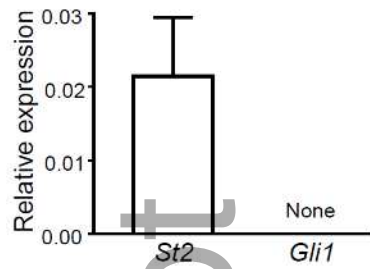
B BDO growth
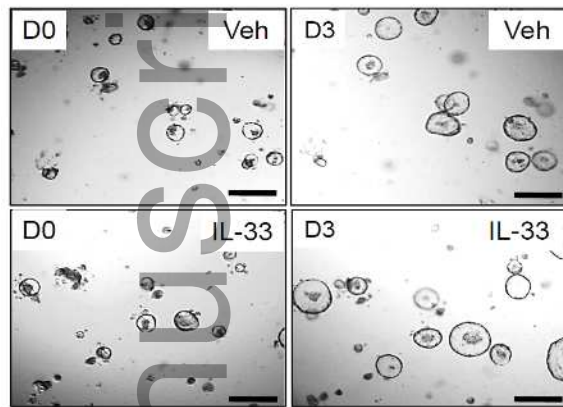
D BDO proliferation

C BDO growth
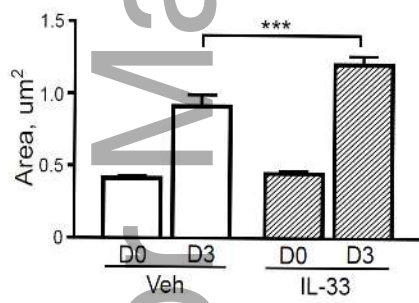
E BDO proliferation

hep4_1295_f7.tif

hep4_1295_f8.tif